INFLUENCE OF MESOSCOPIC FOAM STRUCTURE ON FACE SHEET DEBONDING IN CFRP FOAM CORE SANDWICH PANELS

R. Schlimper[1*], M. John[1], M. Rinker[1], R. Schäuble[1]

[1]*Fraunhofer Institute for Mechanics of Materials IWM, Walter-Hülse-Str. 1, 06120 Halle, Germany*
**ralf.schlimper@iwmh.fraunhofer.de*

Keywords: sandwich structures, fracture mechanics, face sheet debonding, foam structure.

Abstract

The face sheet debonding of CFRP foam core sandwich structures under quasi-static loading is investigated by the Single Cantilever Beam test where the initial crack is loaded under global Mode I condition. The influence of the foam structure on the mesoscopic scale is studied by the use of several grades of Polymethacrylimid (PMI) foam cores varying in density and cell size. The morphological characterization of the foam structure is done by X-Ray computed tomography and 3d image analysis. The measured fracture toughness increases on increasing cell size of the foam core material and indicates enhanced damage tolerance concerning local debonding damages. Unfortunately the structural weight also increases on increasing cell size and related resin absorption of the foam core.

1 Introduction

Sandwich structures consisting of a light foam core and CFRP face sheets with high stiffness and strength provide potential for many light weight applications e.g. in transportation industries like automotive and aviation. The closed cell foam core allows very efficient manufacturing of also complex shaped parts via vacuum assisted resin infusion process (VARI) [1]. Within the process the neat resin infiltrates the dry fibers of the face sheets and fills cut cells on the surface of the closed cell polymer foam core. Hence the interface strength, which is essential for the mechanical performance of a sandwich structure, also depends on the morphological foam structure on the mesoscopic scale, e.g. mean cell size. On the other hand structural weight increases by resin absorption of the cut foam cells. Sandwich structures are prone to impact loads which typically cause local debonding of the face sheets on even low impact velocities. For their use in high loaded safety relevant structures the damage tolerance related to these impact damages which already can occur in the manufacturing process by a tool drop as well as in service by collision with other objects and are barely visible by human eye has to be predictable by engineering methods. According to this need in the recent 20 years a lot of fracture mechanical investigations on sandwich structures with composite face sheets and foam or honeycomb core have been published [2-6, 10,11]. However Up to now there exist no standard for such test on sandwich structures as it is the case for assessment of delamination of composite laminates. That is why the variety of test methods is wide but recently there are some attempts for the standardization e.g. of the so called Single Cantilever Beam (SCB) test [5]. This test is based on the Double Cantilever Beam (DCB) test where the crack is loaded in Mode I loading condition. For sandwich specimens with an initial interface crack and therefore asymmetric beams the test was modified by fixing the lower part of the specimen on a supporting plate. The paper presents systematic investigations on face sheet debonding depending on mesoscopic structure of the foam core by quasi-static SCB testing on sandwich specimens with foam core material varying in cell size and density.

2 Materials and testing methods

2.1 Manufacturing of specimens

Sandwich panels were manufactured via vacuum assisted resin infusion process (VARI), which is a common process for manufacturing of large scale shell like composite sandwich parts, e.g. in aircraft industry [1]. The sandwich panels consist of a Polymethacrylimide (PMI) foam core (ROHACELL® by Evonik Industries AG) and CFRP face sheets. Latter were built by PANEX®35 carbon fibers in UD and biaxial (+45°/-45°) textiles and the epoxy system Biresin CR80 with hardener CH80-6 by the company Sika. The stacking sequence of each face sheet was $[(+45/-45/0)_s]_2$. It leads to a laminate thickness of 2,4 mm after curing. The bending stiffness of the face sheet laminate is 56000 Nmm² per mm width (measured by 4 point bending test). As foam core several grades of the ROHACELL® foam were used, which vary in density and cell size (see table 1). The height of the foam core h_c was 25 mm. According to the used epoxy resin the specimens were infiltrated at room temperature and then cured at 45 °C for 5h.

grade	**density**	**Youngs modulus**
	kg/m³	***MPa***
51 RIMA	52	75
51 RIST	52	75
110 RIST	110	180
51 WF	52	75

Table 1. Material data of ROHACELL® foam core material [7]

2.2 X-Ray computed tomography and 3d image analysis

This investigations were done by the CT-scanner nanome|x 180NF of the company Phoenix x|ray with a 180 kV X-ray source and a digital flat panel detector with a lateral resolution of 512² pixels. The scanning parameters for the acquisition of ca. 1200 projection images were ca. 70 kV, 200 µA. Both sandwich and pure foam specimens with cubic shape and ca. 10 mm edge length were cut from manufactured sandwich panels and scanned by X-Ray CT.

The acquired 3d image data of the mesoscopic foam structure and the face/core interface was analyzed by 3d image processing and analyzing software MAVI [8] to determine morphological parameters e.g. the mean cell size. A more detailed description of the procedure can be found in [9].

2.3 SCB testing

For the quasi-static single cantilever beam (SCB) testing the sandwich specimens (length 330 mm, width 50 mm) were glued to a supporting plate. Load was applied by a piano hinge (edge length d=30 mm) which was glued on the upper side of the specimen (see figure 1) and a joining rod with length 300 mm to prevent the introduction of shear loading into the interface debond. The initial crack with length a_0=50 mm was created by a Teflon film (thickness 50 µm) which partially prevents the face sheet bonding. Three specimens were tested per configuration. Displacement rate was set to 1 mm/min and load-deflection curve was recorded during the test.

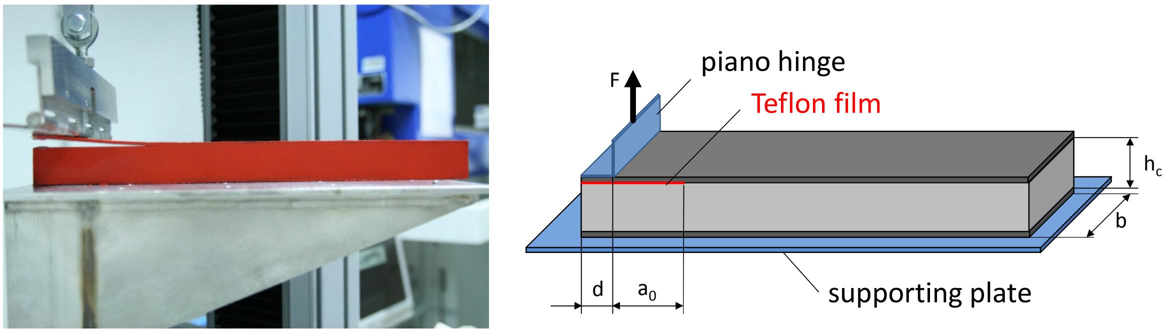

Figure 1. SCB test, photograph (left) and schematic drawing (right)

In additional tests with the same fixture the specimen stiffness was measured in dependency of the crack length which was manually extended step wise between static loading and unloading cycles. During this test the specimen was only loaded in the linear range to avoid autonomous crack growth. Measured stiffness was compared to the analytical solution for the compliance of DCB sandwich specimen given by [10,11] with application to the SCB geometry with the lower part of the specimen fixed on a supporting plate [6] (see figure 1):

$$C = \frac{1}{3D_f}\left[a^3 + 3a^2\eta^{1/4} + 3a\eta^{1/2} + \frac{3}{2}\eta^{3/4}\right] \quad (1)$$

with crack length a, the bending stiffness of the face sheet D_f and $\eta = \frac{2D_f h_c}{bE_c}$ where h_c and E_c are the height and the Youngs modulus of the core and b is the width of the specimen. The comparison of the normalized stiffness related to the initial slope of the force deflection curve of the specimen with initial crack length a_0 shows quite good agreement between experimental data and the analytical model. Hence the analytical model and the so called compliance method were used for calculation of crack length in the static SCB tests because it could not be measured directly on the specimen. Then the energy release rate was determined by:

$$ERR = \frac{F^2}{2b}\frac{\partial C}{\partial a} = \frac{F^2}{2bD_f}\left[a^2 + 2a\eta^{1/4} + \eta^{1/2}\right] \quad (2)$$

3 Results

3.1 Morphological characterization of the foam structure

The 3d images of the pure foam material reveal the polyhedral shaped foam structure of the investigated ROHACELL® foams with thin plane cell walls which meet in struts and vertices. The material concentration in the struts and vertices is small. They are only slightly thicker than the cell walls. The cell sizes in terms of the mean cell diameter determined by 3d image analysis are listed in table 2. The cell size of foam grade 51 RIMA could not properly resolved by the X-Ray CT that is why it was measured by light microscopy on a cut cross section of a foam specimen.

	51 RIMA*	51 RIST	110 RIST	51 WF
mean cell diameter [mm]	0,072	0,389	0,293	0,604
coefficient of variation [%]		17	14	19

Table 2. Mean cell diameter of RHACELL® foams determined by X-Ray CT and 3d image analysis, *except of 51 RIMA, which was analyzed by light microscopy

Figure 2 shows a slice through a 3d image of a face/core interface of a sandwich specimen with 110 RIST foam core and glass fiber reinforced face sheet, which was chosen for a better contrast of the fiber bundles in the image. In all taken images it could be observed that only the first layer of cut foam cells is filled by resin during the VARI manufacturing process. The investigation of the absorbed resin both in terms of the cut foam cells and in terms of segmentation of the resin phase in the 3d images provides similar results and therefore confirms the observation of the filled cut cell layer.

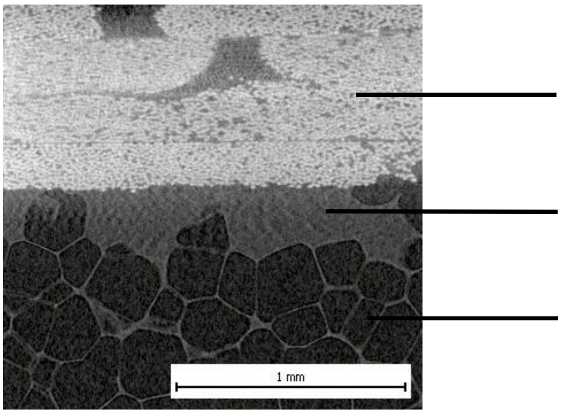

Figure 2. Slice view through 3d image of the interface of an sandwich specimen with 110 RIST foam core

3.2 Compliance method

The interrupted quasi-static SCB test with stepwise manual extension of the crack length provides the stiffness of the specimen in dependency of the crack length. Figure 3 shows the normalized stiffness (related to the initial stiffness of the specimen with initial crack length a_0) of a specimen with 51 RIST foam core which decreases on increasing crack length. The experimental data marked by the squares coincides very well to the analytical model mentioned above and marked by the solid line in figure 3. That legitimates the use of the analytical model for the further examination of the SCB tests to overcome the problem of the unknown crack length by running the test continuously.

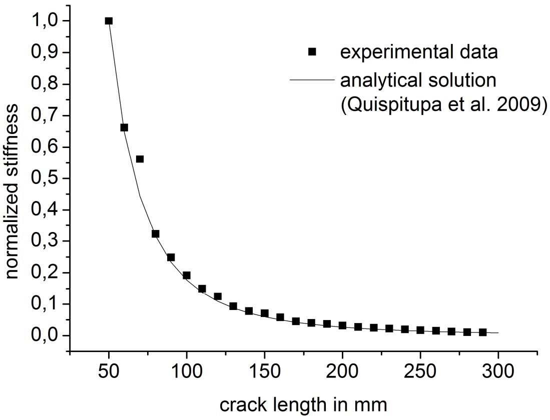

Figure 3. Normalized stiffness vs. crack length of a SCB specimen with 51 RIST foam core

3.3 Quasi-static SCB test

All recorded load-deflection curves show linear behavior up to the maximum load, where the initial crack starts growing and the load drops down. With further deformation the load again increases linear up to the next drop due to crack extension when the critical load is reached. This continues up to the complete debonding of the face sheet (see figure 4, left). Hence quasi static stable crack growth could be observed on all tested specimens. Maximum load and the shape of the load deflection curves of the 3 tested specimens per each sandwich configuration are nearly identical. However the configurations 51 RIST and 51 WF show a more continuous crack growth without the distinct linear slopes in the load deflection curves (see figure 4, right). In all cases the crack grows in the foam core near the face/core interface. A thin layer of foam material could be observed on the debonded face sheets after the test.

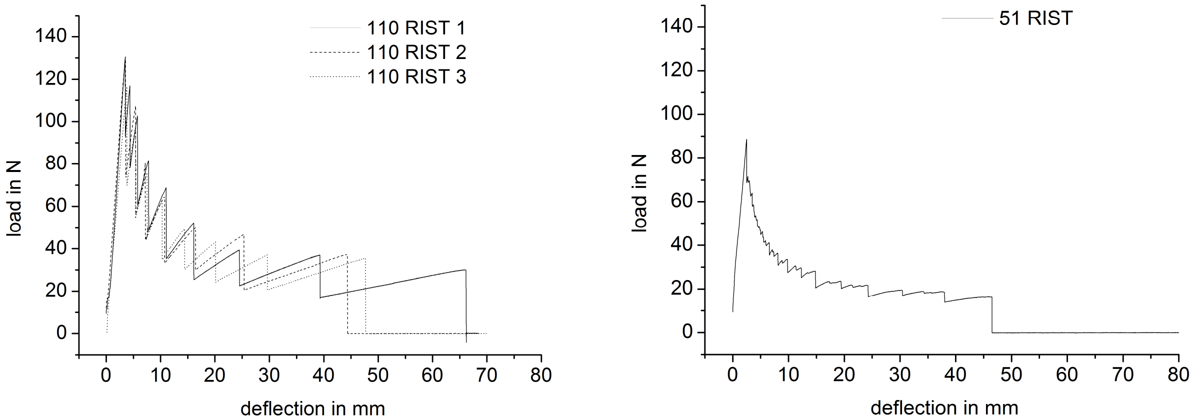

Figure 4. Load-deflection curves recorded during SCB testing on 110 RIST (left) and 51 RIST (right) foam core sandwich specimens

The fracture toughness' were calculated in the point of maximum load with the initial crack length on the one hand and from the whole load-deflection curve on the other. In case of load-deflection curves with distinct linear slopes between the local load maxima the fracture toughness was calculated for each local load maximum with the related crack length given by equation (1) and then averaged over the whole curve and all specimens per each configuration. In case of more continuous load-deflection curves (e.g. 51 RIST, see figure 4 right) the crack lengths were determined via numeric differentiation of the load-deflection curves. The calculated values are given in table 3. On nearly all configurations the fracture toughness calculated from the maximum load is higher than the one calculated from the further load-deflection curve. This was already observed by Rinker et al. [6] who made the position of crack responsible for the difference. While in the beginning of the test the crack is situated in the face/core interface by the application of the Teflon film the crack runs within the foam core near the interface during further progression of the test. Compared to the interface which consist of resin filled foam cells the fracture toughness of the pure foam material is assumed to be smaller and results in smaller measured fracture toughness during this kind of test. One further reason for the difference is the shape of the initial crack which is not an ideal sharp crack although the applied Teflon film was only 50 µm thin.

configuration	**ERR_{C_Fmax}** ***N/mm***	**ERR_C** ***N/mm***
51 RIMA	0,053	0,052
51 RIST	0,126	0,080
110 RIST	0,231	0,195
51 WF	0,244	0,145

Table 3. Critical **e**nergy release rates determined on the tested sandwich configurations, ERR_{C_Fmax} calculated with maximum load and initial crack length, ERR_C calculated from the whole force deflection curve

3.4 Influence of cell size and foam stiffness

Figure 5 shows that interface strength is strongly influenced by the mechanical properties of the foam core on the one and morphological structure, namely cell size on the other hand.

Figure 5, left shows the determined fracture toughness versus density of foam core material ROHACELL® RIST with the same cell size. The mechanical properties, e.g. stiffness and strength of the foam material are principally related to the foam density. Both the ERR_{C_Fmax} calculated on maximum load and ERR_C calculated from the whole load-deflection curve are ca. double in case of double foam density. The standard deviation plotted by the error bars increases on increasing fracture toughness.

Figure 5, right shows the determined fracture toughness versus the mean cell diameter of the foam core materials with constant density (52 kg/m³) and therefore similar stiffness and strenght. As expected the fracture toughness increases on increasing cell diameter. But in this diagram the ERR_{C_Fmax} calculated from the maximum load increases much more than the ERR_C calculated from the whole load-deflection curve. However both values are nearly identical on the ROHACELL® 51 RIMA foam with the smallest cell size. This confirms the assumptions made in the section above concerning the difference between the two ways for determining the fracture toughness from measured SCB test data. In case of 51 RIMA the thickness of the Teflon film nearly coincides with the mean cell size and the crack immediately grows in the foam material. However in the other tested foam materials the initial artificial crack tip is situated in the layer of resin filled foam cells, which diameters are a multiple of the thickness of the Teflon film. In the latter case the fracture toughness calculated from the maximum load is a parameter which characterizes the strength of the face/core interface more than the fracture toughness calculated from the whole load-deflection curve. It is mainly affected by the cell size and hardly by the foam stiffness or strength as shown in figure 5.

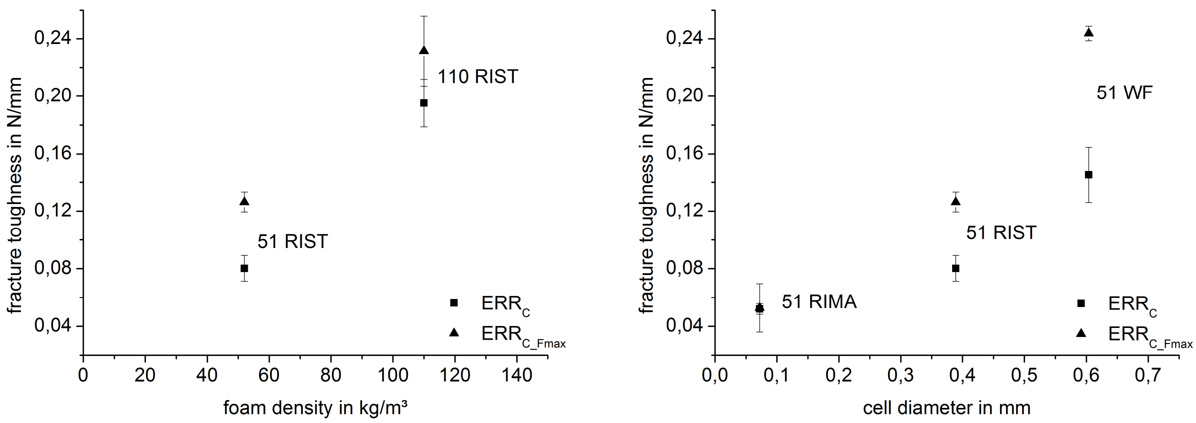

Figure 5. Face/core interface fracture toughness in dependency of foams density (left) and cell size of the foam core (right)

4 Conclusion

The investigation presented in the paper provides results concerning the fracture mechanical assessment of the face/core interface of CFRP foam core sandwich structures loaded under global mode I condition. The SCB test was applied to sandwich specimens with several foam core materials differing in density and cell size to evaluate the interface strength comparative in terms of the fracture toughness. The morphological investigations also presented in the paper allow conclusions about the correlation between the mesoscopic structure of the foam core material and the interface strength.

It could be shown that the resistance against interface crack propagation under static condition is affected by both the mechanical properties and the cell size of the foam core material. However during all tests the crack propagates in the cell layer adjacent to the filled cut cell layer, which represents the face/core interface and is therefore only a quasi interface crack, which still covers the scenario of impact damage in a sandwich structure, where the face sheet locally debonds from the foam core. The reason for that is the higher fracture toughness of the resin filled cell layer compared to that of the pure foam material, which was indicated by the difference between the fracture toughness calculated with the load maximum and the one calculated from the whole load-deflection curve. The latter was found to be 15 to 40 % smaller, because after reaching the maximum load the crack runs in the foam core near the interface. For further investigations of this problem the determined interface fracture toughness' have to be compared with the fracture toughness of the pure foam material which can be measured by the SENB (Single Edge Notched Bending) test as described in [12].
By plotting the determined fracture toughness' versus the weight of the tested sandwich panels one can compare several foam core materials with varying density and cell size in terms of the weight of the sandwich panel and the interface fracture toughness (see figure 6). An optimized sandwich structure in terms of weight and damage tolerance related to debonding damages, e.g. in consequence of an impact, would be found in the upper left corner of this diagram.

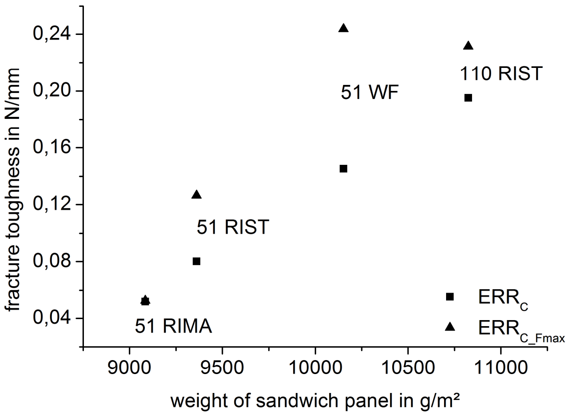

Figure 6. Fracture toughness of all tested sandwich configurations versus weight of the sandwich panel

Acknowledgement

The authors want to acknowledge the company Evonik Industries AG especially Dr. A Roth and F. Goldmann for kindly providing the material for the investigations.

References

[1] Zahlen P.C., Rinker M., Heim C. *Advanced Manufacturing of Large, Complex Foam Core Sandwich Panels* in Proceedings of *8th International Conference on Sandwich Structures*, Porto, Portugal, (2008)

[2] Burman M. Fatigue *Crack Initiation and Propagation in Sandwich Structures*. PhD thesis, *Department of Aeronautics, Royal Institute of Technology*, Stockholm, Sweden, (1998)

[3] Shipsha A., Burman M., Zenkert D. Interfacial fatigue crack growth in foam core sandwich structures. *Fatigue & Fracture of Engineering Materials & Structures*, **Vol. 22**, pp. 123-131, (1999)

[4] Berkowitz C.K., Johnson W.S. Fracture and fatigue tests and analysis of composite sandwich structure. *Journal of Composite Materials*, **Vol. 39**, pp. 1417-1431, (2005)

[5] Ratcliffe J.G., Reeder J.R. Sizing a single cantilever beam specimen for characterizing facesheet/core peel debonding in sandwich structure. *Journal of Composite Materials,* **Vol. 45 No. 25**, pp. 2669-2684 (2011)

[6] Rinker M. et al. Face sheet debonding in CFRP/PMI sandwich structures under quasi-static and fatigue loading considering residual thermal stress. *Engineering Fracture Mechanics*, **Vol. 78 No 17**, pp. 2835-2847 (2011)

[7] Evonik Industries AG Performance Polymers. *Material Data Sheet*, loaded from www.rohacell.com on April 2012.

[8] Fraunhofer ITWM: MAVI - Modular Algorithms for Volume Images, (2009), URL http://www.itwm.fhg.de/mab/projects/MAVI

[9] Schlimper R., Müller M., Willner F., Rinker M., Schäuble R., *Resin absorption and deformation behaviour of foam core materials for high performance sandwich panels* in Proceedings of *14th European Conference on Composite Materials*, Budapest, Hungary, (2010)

[10] Avilés F., Carlsson L.A. Analysis of the sandwich DCB specimen for debond characterization. *Journal of Engineering Fracture Mechanics,* **Vol. 75 No. 2**, pp. 153-168 (2008)

[11] Quispitupa A., Berggreen C., Carlsson L.A. On the analysis of a mixed mode bending sandwich specimen for debond fracture characterization. *Journal of Engineering Fracture Mechanics*, **Vol. 76 No. 4**, pp. 594-613 (2009)

[12] John M., Rinker M., Schäuble R. *Bruchmechanische Kennwertermittlung an Polymethacrylimid-Hartschäumen* in Proceedings of *12. Tagung Problemseminar Deformation und Bruchverhalten von Kunststoffen*, Merseburg, Germany; (2009)